# Study of Two-Phase Microslug Formation in a Microchannel Cross Junction

M. Ryan McDevitt[*,1], Darren L. Hitt[1] and Justin W. McCabe[1]
[1]The University of Vermont, Burlington, VT
*Corresponding author: ryan.mcdevitt@uvm.edu

**Abstract:** NASA and the Department of Defense have interest in the development of satellites, which are several orders of magnitude smaller than those currently in use. These 'nanosats' will require new propulsion systems to offer precise thrust and impulse-bit characteristics on the order of 10-100 μN and 100-1000 μN•s respectively. To meet these demands, a pressure-driven MEMS-based monopropellant thruster has been proposed by NASA GSFC [1]. In this system, microscopic fluid slugs, or 'microslugs', are generated by converging the fuel with an inert gas at a 4-way 90° cross-junction within a microchannel as shown in Figure 1. By controlling the size and frequency of these fuel microslugs, the resulting thrust and impulse-bit characteristics can meet the design requirements.

The goal of the present study is the creation of a numerical model to characterize the microslug formation phenomenon. The level set method as implemented in COMSOL Multiphysics 3.5a was used to track the interface between the two fluids. The simulations were able to capture the underlying physics of the formation process, and will allow for further parametric studies that will aid in the design and optimization of the microscale thruster.

**Keywords:** Two-phase, Level Set, Microfluidics

## 1. Introduction

NASA and the Department of Defense agencies have expressed interest in using "nanosats," or satellites featuring a mass <20 kg for the next generation of space missions. The nanosats will be capable of operating in distributed networks ('formation flying') and performing mission objectives not currently achievable with traditional satellite architectures. As a result of the dramatically reduced size, nanosats will require unique propulsion systems to provide the levels of thrust/impulse required for orbital maneuvering and precise station-keeping [1], [2]. Specifically, thrust levels of O(μN) and impulse bits of approximately 1-100 μN·s are expected as design parameters. Reviews of micropropulsion strategies for nanosat microthrusters can be found in Mueller [3] and Reichbach et al. [4].

Monopropellant propulsion is an attractive scheme for microthruster applications since it offers a combination of high energy density and simplicity of design. The latter is especially significant for the construction of miniaturized propulsion systems. The first prototype monopropellant microthruster reported in the aerospace literature was developed using microelectromechanical systems (MEMS) techniques at NASA/Goddard Space Flight Center [5].

The typical operation of a microthruster consists of the delivery of a specified amount of impulse to the spacecraft and is thus inherently transient in nature. For a monopropellant microthruster (indeed, any chemical microthruster) this involves the throttling of the propellant via a microvalve. During the shutdown process there will be an unavoidable residual thrust resulting from the finite actuation of the valve and, for micropropulsion applications, the impact of the associated residual impulse may be significant. For example, it has been determined from numerical simulations of the NASA/GSFC prototype operation shown that the residual thrust produced during the shutdown of the thruster may lead to a residual impulse which is more than twice the design impulse bit [6].

Given the potentially troublesome throttling issues associated with MEMS-based microthruster designs, it would be highly desirable to have an alternative method capable of producing 'discrete' impulses for attitude control and adjustment. Indeed, such a scheme already exists for solid propellants in the DARPA 'digital microthruster' [7].

In this study we examine a microfluidic technique intended to produce the 'digital propulsion' effect with a liquid monopropellant

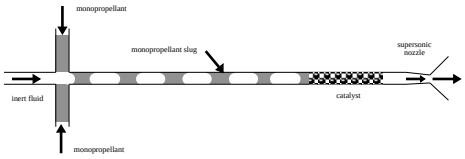


**Figure 1** Schematic of Proposed Monopropellant Thruster

and inert gas, which was first reported in [8]. The key features of the design are depicted in Fig. 1. A liquid monopropellant and a second immiscible, inert fluid converge at a microscopic junction. The inert gas pinches off at the junction in a precise and repeatable manner, leaving slugs of liquid monopropellant between them. The array of monopropellant slugs flow through the outlet channel where they undergo a chemical decomposition in an *in situ* catalyst bed. This will be embedded directly into the channel thereby simplifying the geometry as well as decreasing the footprint on the chip. The inert fluid will pass through the bed chemically unaffected. The decomposition products then flow directly into a supersonic nozzle to convert the thermal energy into kinetic energy to produce the specified thrust.

While conceptually straightforward, the actual operation will depend principally upon the characteristics of the monopropellant slugs, which are formed. Recent studies in the microfluidics literature have demonstrated that two immiscible liquids at a microscopic T-junction can be used to create slug structures that are periodic and highly repeatable. [10]-[11] While these studies provide a foundation for further research they are limited in practical application due to the need to carry a second pressurized liquid on the satellite. The efficiency of the catalytic process in generating thermal energy may also be decreased due to the need to heat the inert fluid. In addition, if the secondary fluid is an oil, fouling may occur in the catalyst bed. Work has been performed by Cubaud et al. [12]- [13] for gas-liquid flows in larger microchannels O[100 μm]. Using an inert gas will decrease the total mass budget for the propulsion system. In McCabe et al. [8], a pressure-driven system which was an order of magnitude smaller than that described in Cubaud *et al*. [13] was created to characterize the microslug formation by the inlet pressure ratio. They found that controlling the pressure ratio at the inlets allowed them to create steady, periodic microslugs of different sizes and lengths. To apply these findings to the creation of a microthruster, more information is needed about the effects of materials properties on the microslug formation.

The goal of this study is to create a numerical model of a microchannel junction, using the level set method to track the gas-liquid interface. This simulation will help to characterize the slug length and frequency by the inlet parameters, and will serve as the basis for further numerical studies into the microslug formation process.

## 2. Methodology

A 2D model of the microchannel junction was created, using the level set method to track the interface between the two phases and flow visualization experiments were performed to verify the numerical results. For this study, $H_2O$ has been used in lieu of actual $H_2O_2$ since its properties are similar and we do not wish to incur any reaction at this stage of the work. In future work $H_2O_2$ will be used. Air is used instead of a chemically inert gas such as Ar or $N_2$. The predominant flow properties in microfluidic flow analysis are surface tension and viscosity. As $H_2O$ and air exhibit very similar microfluidic properties to their analogues, the two substitutions should not present any fundamental differences in the measurements.

### 2.1 Mathematical Model

A standard approach for tracking the interface between two immiscible fluids is to calculate the flow field using the incompressible, unsteady Navier-Stokes equations and track the movement of the interface by an auxiliary method. These methods include Volume of Fluids (VOF), Level Set and Front-Tracking methods. For this simulation, the level set method was selected for its accuracy of tracking the interface between the two fluids. A modified version of this method is implemented in COMSOL v3.5a (MEMS-module), which improves the mass conservation of the level set. In this software, the Navier-Stokes equations are solved along with the level set equation, shown in Eq. 1 where $\gamma$ represents a re-initialization parameter and $\varepsilon$ represents an

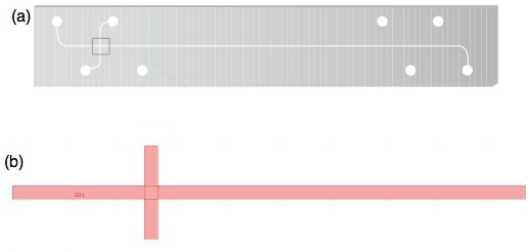


**Figure 2** (a) Microchannel Layout (b) Computational Domain

estimated interface thickness as described in [14]. For numerical stability, the minimum mesh size should be O[ε] and γ should be roughly equivalent to the maximum velocity of the flow.

$$\frac{\partial \phi}{\partial t} + \mathbf{u} \cdot \nabla \phi = \gamma \nabla \cdot (\varepsilon \nabla \phi - \phi(\mathbf{1} - \phi) \frac{\nabla \phi}{|\nabla \phi|}) \quad (1)$$

The density and dynamic viscosity are then solved using Eqns.(2,3).

$$\rho = \rho_1 + (\rho_2 - \rho_1)\phi \quad (2)$$

$$\nu = \nu_1 + (\nu_2 - \nu_1)\phi \quad (3)$$

This program was used to model a reduced version of the computational domain as shown in Fig. 2. As implemented in COMSOL, the level set method requires a re-initialization value to ensure that the interface remains conserved. This interface is displayed in Fig. 3.

**Figure 3** Initial Interface

### 2.2 Boundary Conditions

The physical system to be simulated is fully pressure-driven, but the simulation is more stable when velocity boundary conditions are used. To model the system, $U_L$ (superficial liquid velocity) and $U_G$ (superficial gas velocity) were found using Poiseulle's Law:

$$\Delta P = Q R_h \quad (4)$$

where $R_h$ is based on the specific geometry of the system. As an approximation, the system is assumed to be parabolic with a base of 50 μm and a height of 20 μm. With this assumption, $R_h$ can be approximated as:

$$R_h = \frac{105}{4} \mu_L L (\frac{1}{bh^3}) \quad (5)$$

where L is the length of the channel. If the total pressure drop across the system is assumed to be known, then Eq 4 can be rearranged to find the volumetric flow rate, Q. Using the cross-sectional area, the velocity can be found by:

$$V = \frac{\frac{\Delta P}{R_h}}{\frac{2}{3} bh} \quad (6)$$

This velocity is then used as the inlet condition for the air and water phases.

### 2.3 Grid Generation and Convergence

COMSOL implements the Level Set method as a smooth step function between 0 and 1, where the .5 isocontour represents the actual interface. To accurately model multiphase flow, the grid must be smaller than the projected interface thickness at all locations that it may travel. A grid convergence study found that a grid size of 3.33 μm resulting in 187,969 cells, is able to capture the interface with the least amount of computational overhead. A larger grid size causes the interface to smear, which results in non-physical flow patterns.

### 2.4 2D vs. 3D Simulations

Due to the intense computational demands of simulating the flow in 3D, using a 2D simulation was desirable. In Qian and Lawal [15], a strong connection between the 2D and 3D simulations of micro-slug generation in micro-channels was found. To verify that a similar connection exists in this study, a 3D model of the junction was simulated and compared against the 2D model. The original models showed a discrepancy, but this was corrected by adding a "shallow channel" term:

$$\vec{F}_\eta = \frac{12\eta\vec{u}}{h^2} \quad (7)$$

where $\vec{F}_\eta$ represents a body force resulting from the channel top and bottom. This quasi-3D flow compares very closely to the full 3D simulation and verifies that a 2D simulation, with this shallow-channel term, is appropriate for simulating the flow.

### 2.5 Experimental Apparatus

To verify the accuracy of the numerical simulations at standard inlet conditions, flow visualization experiments were run. These were done with a pressure driven microfluidic flow system using compressed air and pressurized DI water that has been designed at the microfluids lab at the University of Vermont. The microfluidic chip, which contains the flow channels, is manufactured offsite by Micralyne Inc. The chip is made of Schott Borofloat glass, which allows for straightforward optical analysis. The chip contains four access holes three of which lead to channels that merge into a 90° junction and a fourth serves as the outlet. The chip layout is shown in Fig. 4a. The channel cross section is shown in Fig. 4b. The width of the mask line ($W_{maskline}$ in the figure) is 10µm. This leads to a maximum channel width of 50µm and a channel depth of 20µm.

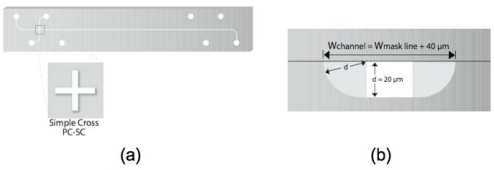


**Figure 4** (a) Schematic of Microchannel Layout (b) Schematic of Microchannel Cross-Section

Tubing is connected via threaded ports mounted to the glass directly above the access holes. Fig. 5 shows the arrangement of the system. Compressed air supplies the air line as well as the pressure for the water reservoir. Digital manometers are used to obtain pressure readings at the air and water reservoirs. Two precision miniature regulators control the pressures at each of the three inlets. The water pressure in each of the two water lines must be equal at the inlet

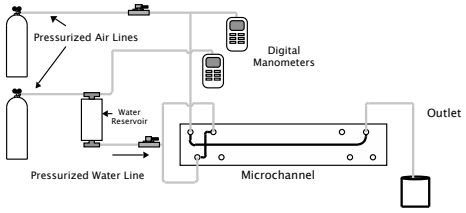


**Figure 5** Schematic of the Pressure Driven Microfluidic System

ports for the system to exhibit the desired flow patterns. This is done by limiting the pressure drops due to flow resistance before the two inlet ports. The compressed air is initially filtered to 7 µm and each water line is again filtered using 2 µm micro-filters to eliminate any clogging in the microchannel, which may lead to a pressure drop causing a bias in the system. The base pressure of the system is set by the water pressure and the air pressure is ranged from .5 psi below the base pressure to .5 psi above in steps of .2 psi. The lower limit of the air pressure corresponds to entirely water in the outlet channel. The upper limit is the point at which the slug formation becomes unstable resulting in a transition region between slug flow and annular flow, the latter being unacceptable for our application. Cubaud et al. shows the transition regions on a two-phase flow pattern map.

Flow visualization is achieved using an InfiniTube In-Line video system equipped with a fiber optic light source and a high speed CCD camera. Digital video of slug formation is captured at rates up to 3900 frames per second with exposure times as low as 75 µs. The resolution is 80×80 pixels when measuring the slug frequency and size at the higher limit of the base pressure range. The image sequences are then processed and analyzed using in-house MATLAB codes.

## 3. Results

The numerical model was compared against the experimental flow visualization to demonstrate its accuracy. Figure 6 shows a similarity between the downstream pinchoff mechanism seen in the experiments and the simulations at similar inlet pressure ratio. It takes the formation of a few microslugs before the pinchoff location

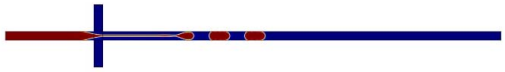

(a) NUMERICAL SIMULATION

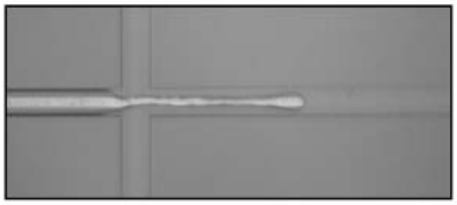

(b) EXPERIMENTAL RESULTS

**Figure 6** Comparison of Numerical and Experimental Results

stabilizes; this process is shown in Fig. 7. This phenomenon, which is not captured in the flow visualization experiments, occurs very quickly. The slugs first appear very close to the junction but the pinchoff location continues to travel downstream until it reaches a steady location ≈ 7 channel widths downstream. Once this location has been reached, slugs are generated in a steady, periodic fashion at regular intervals.

Varying the inlet conditions results in a range of flow regimes that have been shown in [8]- [13] including dripping, jetting and annular flow. This study is focused on the regime around 30 psi as this would result in the desired microthruster characteristics.

## 4. Discussion

The slug generation has been characterized by the ratio of the inlet pressures ΔP. Of particular interest is the breakup mechanism shown in these simulations. In Cubaud and Mason [16] a range of flow regimes were characterized for liquid-liquid flows with high viscosity ratios (24-1484). They found that as the Ca number dropped (through a lowering of the inlet flow rates) the flow regime transitioned from annular to ”jetting” to ”dripping”. In annular flow, there is no microslugs and thus no detachment point. In the jetting regime, the flow exhibits capillary instability and breaks up far downstream (5-15 channel widths). Lowering the inlet velocity further leads to dripping which is the classic Taylor flow regime that has been well-described [13]. In this mechanism the geometric constraints of the channel cause the flow to squeeze into microslugs.

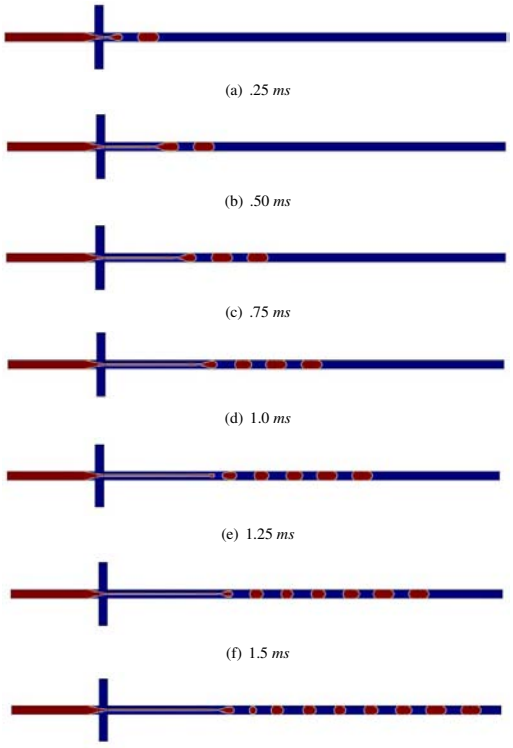

(a) .25 *ms*

(b) .50 *ms*

(c) .75 *ms*

(d) 1.0 *ms*

(e) 1.25 *ms*

(f) 1.5 *ms*

(g) 1.75 *ms*

**Figure 7** Evolution of Pinchoff Location

The flow regime exhibited in these simulations, for the inlet pressures used (30psi, ΔP = .3psi) appears to be similar to the jetting regime described by Cubaud and Mason [16]. After the transient startup, where the slugs are generated very near the junction, the flow detachment point reaches a steady location (≈ 7 channel widths downstream) where the microslugs continue to be generated. This closely matches the pinchoff mechanism that was seen in the flow visualization experiments.

## 5. Conclusions

In this study, we have used numerical techniques to examine the generation of microslugs at a 4-way junction as the basis of a discrete monopropellant-based fuel delivery system for a nanosat. This intended micropropulsion application drove the channel geometry and dimensions, the material properties of the fluids used as well as the flow control system and inlet parameters. A quasi-3D model of the microchannel junction was created and simulated using velocity boundary conditions that

correspond with the desired operating conditions of the microthruster. A flow visualization experiment was run to verify the flow regime that was seen in the simulations.

The goal of these simulations was to apply the level set method to modeling microslug formation at a microchannel junction. Within the reduced computational domain created, this was only possible when the pressure boundary conditions were converted to velocity boundary conditions using analytical methods. This process results in flow regimes that are qualitatively similar to the experimental results, but show differences in the microslug size and formation frequency. These results point to the promise of using the level set method, and justify further refining the model to eliminate the inaccuracies.

## 8. References


1. Blandino, J. and Cassady, R., 1998, "Propulsion requirements and options for the New Millennium Interferometer (DS-3) Mission," *AIAA Paper 98-3331, Proceedings of the 34th AIAA/ASME/SAE/ASEE Joint Propulsion Conference & Exhibit, Cleveland, OH.*

2. Pollard, J., Chao, C. and Janson, S., 1999, "Populating and Maintaining Cluster Constellations in Low-Earth Orbit," *AIAA 99-2871, Proceedings of the 35th AIAA/ASME/SAE/ASEE Joint Propulsion Conference & Exhibit, Los Angeles, CA, June.*

3. Mueller, J., 2000, "Thruster options for microspacecraft: a review and evaluation of the state-of-the art and emerging technologies, in Micropropulsion for Small Spacecraft", *Progress in Astronautics and Aeronautics*, M. Micci and A. Ketsdever, eds., **Volume 187**, AIAA, Reston, Va., p. 45-137.

4. Reichbach, J., Sedwick, R. and Martinez-Sanchez, M., 2001, "Micropropulsion system selection for precision formation flying satellites," *AIAA 2001-3646, 37th AIAA/ASME/SAE/ASEE Joint Propulsion Conference & Exhibit, Salt Lake City, UT.*

5. Hitt, D., Zakrzwski, C. and Thomas, M., 2001, "MEMS-Based Satellite Micropropulsion Via Catalyzed Hydrogen Peroxide Decomposition," *J. Smart Mater & Struct.*, **Volume 10**, pp. 1163-1175.

6. Kujawa, J. and Hitt, D., 2004, "Transient Shutoff Simulations of a Realistic MEMS Supersonic Nozzle," *Proceedings of the 40th AIAA/ASME/SAE/ASEE Joint Propulsion Conference & Exhibit, Ft. Lauderdale, FL, July.*

7. Lewis, D., Janson, S. and Cohen, R., 2000, "Digital Micro-Propulsion Project," *Sensors & Actuators*, **Volume 80**, pp. 143-54.

8. McCabe, J. and Hitt, D. "Monopropellant Fuel Injection Using Two-Phase Microslug Formation"

9. Dreyfus, R., Tabeling, P. and Williaime, H., 2003, "Ordered and Disordered Patterns in Two-Phase Flows in Microchannels," *Phys. Rev. Let.*, **Volume 90**, No. 14, pp. 14405/1 -4.

10. Harris, T., Hitt, D. and Macken, N., 2003, "Periodic Slug Formation in Converging Immiscible Microchannel Flows," *Bulletin of the American Physical Society*, **Volume 48,** No. 10, p. 58.

11. Harris, T., Hitt, D. and Jenkins, R., 2005, "Discrete Micro-Slug Formation for Micro-Thruster Propellant Delivery" *AIAA Paper 2005-0676*

12. Cubaud, T. and Ho, C., 2004, "Transport of bubbles in square microchannels," *Physics of Fluids*, **Volume 16**, No 12, pp. 4575-85.

13. Cubaud, T., Tatineni, M., Zhong, X. and Ho, C., 2005, "Bubble dispenser in microfluidic devices," *Phys. Review E*, **Volume 72**, 037302.

14.COMSOL AB., 2008, COMSOL Multiphysics Version 3.5a, User's Guide and Reference Guide. Stockholm.

15. Qian, D., Lawal, A. "Numerical study of gas and liquid slugs for Taylor flow in T-junction microchannel," *Chemical Engineering Science*, **Volume 61**, 2006, pp. 7609-25.

16. Cubaud, T., Mason, T. "Capillary threads and viscous droplets in square microchannels," *Physics of Fluids*, **Volume 20**, pp. 1064-75.

## 9. Acknowledgements

This work was supported by the U.S. Air Force Office of Sponsored Research (AFOSR) under Grant # FA9550-06-1-0364 and by NASA Shared Services Center (NSSC) under Grant # NNX09AO59.10.